

A model for the generation of localized transient $[\text{Na}^+]$ elevations in vascular smooth muscle

Nicola Fameli,[†]Kuo-Hsing Kuo, Cornelis van Breemen
*Department of Anesthesiology, Pharmacology and Therapeutics
The University of British Columbia*

Abstract

We present a stochastic computational model to study the mechanism of signalling between a source and a target ionic transporter, both localized on the plasma membrane (PM) and in intracellular nanometre-scale subplasmalemmal signalling compartments comprising the PM, the sarcoplasmic reticulum (SR), Ca^{2+} and Na^+ transporters, and the intervening cytosol. We refer to these compartments, sometimes called junctions, as cytoplasmic nanospaces or nanodomains. In the chain of events leading to Ca^{2+} influx for SR reloading during asynchronous Ca^{2+} waves in vascular smooth muscle (VSM), the physical and functional link between non-selective cation channels (NSCC) and $\text{Na}^+/\text{Ca}^{2+}$ exchangers (NCX) needs to be elucidated in view of two recent findings: the identification of the transient receptor potential canonical channel 6 (TRPC6) as a crucial NSCC in VSM cells and the observation of localized cytosolic $[\text{Na}^+]$ transients following purinergic stimulation of these cells. Having previously helped clarify the Ca^{2+} signalling step between NCX and SERCA behind SR Ca^{2+} refilling, this quantitative approach now allows us to model the upstream linkage of NSCC and NCX. We have implemented a random walk (RW) Monte Carlo (MC) model with simulations mimicking a Na^+ diffusion process originating at the NSCC within PM-SR junctions. The model calculates the average $[\text{Na}^+]$ in the nanospace and also produces $[\text{Na}^+]$ profiles as a function of distance from the Na^+ source. Our results highlight the necessity of a strategic juxtaposition of the relevant signalling channels as well as other physical structures within the nanospaces to permit adequate $[\text{Na}^+]$ build-up to provoke NCX reversal and Ca^{2+} influx to refill the SR.

Keywords: calcium oscillations, calcium signaling, sodium transient, vascular smooth muscle, sarcoplasmic reticulum, stochastic model, monte carlo, random walk, computational model, TRPC6, $\text{Na}^+/\text{Ca}^{2+}$ exchanger.

[†]Corresponding author. Address: 2176, Health Sciences Mall, Vancouver, B. C., Canada V6T 1Z3
tel 1-604-8226198; fax 1-604-8226012. email: fameli@interchange.ubc.ca

1 Introduction

We are not used to thinking of ionic sodium (Na^+) as a *signalling* ion, despite its known relevance for vascular disease. On the other hand, the importance of the second messenger Ca^{2+} in signalling cell function is undisputed. There is however recent experimental evidence supporting the idea that this important species has, at least in vascular smooth muscle cells (VSMC), an almost equally important signalling partner in Na^+ [1, 2], particularly in signalling events that are allowed by the juxtaposition of signalplexes and transporter carrying membranes at nanometric distances from one another. This observation, and others outlined below, as well as a wealth of accumulated knowledge on Na^+ and Ca^{2+} transporters in VSMC has prompted us to take a more quantitative look at the question of Na^+ -related signalling in PM-SR cytoplasmic nanospaces (also referred to as nanodomains or junctions): nanometre-scale signalling compartments comprising the PM, the sarcoplasmic reticulum (SR), Ca^{2+} , Na^+ and other ionic transporters (channels, exchangers and pumps) and relevant signalplexes therein, and the intervening cytosol.

In this article we present a quantitative model aimed at elucidating the mechanism of selective (or site-specific) signalling between a source ionic transporter and a target ionic transporter, both of which are localized on the same membrane and are part of a nanodomain. We developed this model using a stochastic method based on the simulation of ionic diffusion by random walks (RW) within nanospaces modeled according to experimental observations. Here we concentrate on the specific example of a Na^+ transporter, typically a NSCC and a NCX as its target. Generally, during these events Na^+ entry via a NSCC generates a large $[\text{Na}^+]$ gradient, which, in turn, enables reversal of a NCX (presumably in the vicinity of the NSCC) and consequent NCX-mediated Ca^{2+} entry into the subplasmalemmal nanodomain. A few examples highlighting the biological importance of this intra-membrane system and its link to pathogenic mechanisms are (table 1 summarizes these cases): **1)** A critical subplasmalemmal step in the Ca^{2+} signalling cascade giving rise to VSM cell contraction following G-protein coupled receptor adrenergic stimulation[3]—where blocking NCX reversal causes attenuation and elimination of Ca^{2+} oscillations due to impairment of SR refilling; replacement of $[\text{Ca}^{2+}]_i$ oscillations with a tonic Ca^{2+} signal causes a dramatic decrease in smooth muscle force development[4]; in pulmonary artery SM, upregulation of the NCX and Ca^{2+} entry via reverse NCX action is considered one of the mechanisms behind elevated $[\text{Ca}^{2+}]$ in idiopathic pulmonary arterial hypertension patients[5]; **2)** Receptor activated Na^+ entry may also induce NCX reversal in endothelial cells (EC) and this, in turn, gives rise to selective Ca^{2+} -stimulated eNOS activity and NO production; eNOS derived NO is an important physiological vasodilator agent and is accepted as an independent marker of vascular health[6, 7]; in EC NCX operating in forward mode is also important in regulating both $[\text{Ca}^{2+}]_i$ and $[\text{Ca}^{2+}]_{\text{SR}}$; this suggests that local $[\text{Na}^+]_i$, besides the cell membrane potential and the equilibrium potential of the NCX, have a role in the regulation of forward NCX too[8, 9]; **3)** In nerve terminals, a transient $[\text{Na}^+]$ increase linked to a tetanic pulse of the action potential can reverse the NCX to induce presynaptic potentiation; this observation implies a role for the NCX in synaptic facilitation and has consequences for short term memory from reverse NCX malfunction[10, 2]; **4)** In skeletal muscle NCX plays an important role in Ca^{2+} homeostasis, operating in forward as well as reverse mode in that function; $\text{Na}^+/\text{Ca}^{2+}$ exchange is involved in the control of muscle fatigue and there are reports supporting the notion that the beneficial role of external Ca^{2+} in protecting slow-contracting

System	NCX mode/function	Function	References
VSM	rev/SR refilling during ACaW	blood flow	[3]
PASM	rev/NCX upregulation	blood flow	[5]
EC	rev and fwd/eNOS activity	NO production regulation	[6]
nerve	rev/tetanic pulse of action potential	short memory	[10, 2]
skeletal muscle	rev/Ca ²⁺ influx	muscle fatigue	[11]

Table 1: Sampling of systems in which NCX modes are linked to pathologies. Legend: rev=reverse mode (Ca²⁺ influx); fwd=forward mode (Ca²⁺ efflux); ACaW=Asynchronous Ca²⁺ waves; PASM=pulmonary artery smooth muscle; EC=endothelial cells.

soleus muscle against high-frequency fatigue depends mostly on Ca²⁺ influx through reversal of the NCX[11]; **5)** although the role of NCX in heart is still poorly understood, both its Ca²⁺-efflux and influx modes are observed in cardiac myocytes and the latter is likely a consequence of subplasmalemmal Na⁺ elevations[12].

All of the above emphasize that modulation of Ca²⁺ signaling via Na⁺ and Na⁺/Ca²⁺ exchange is of great clinical relevance in areas such as hypertension, chronic heart failure and possibly cerebral and skeletal muscle malfunction.

This study sheds new light on a few new scientifically interesting key factors regarding the “workings” of intracellular signalling nanospaces. We investigate the role, and importance, of having a confining surface, namely another lipid membrane, facing the membrane where the source and target transporters belong. This emerges as an important feature of nanodomains, as previous observations had hinted[13, 14], but it would appear that it alone cannot be entirely responsible for the generation of a sufficiently large local [Na⁺] transient elevations. We find that to understand how sufficient [Na⁺] can be built up within the nanodomain to trigger NCX reversal and Ca²⁺ signalling downstream, it is important to account for other factors such as the role of physical obstructions to Na⁺ diffusion and the possible organization of these obstructions.

2 Methods

2.1 Electron microscopy

Details of the electron microscopy have been described previously[15]. The primary fixative solution contained 1.5% glutaraldehyde, 1.5% paraformaldehyde and 1% tannic acid in 0.1 M sodium cacodylate buffer that was pre-warmed to the same temperature as the experimental buffer solution (37 °C). The rings of rabbit IVC were fixed at 37 °C for 10 minutes, then dissected into small blocks, approximately 1 mm×0.5 mm×0.2 mm in size and put in the same fixative for 2 h at 4 °C on a shaker. The blocks were then washed three times in 0.1 M sodium cacodylate (30 min). In the process of secondary fixation, the blocks were post-fixed with 1% OsO₄ in 0.1 M sodium cacodylate buffer for 1 h followed by three washes with

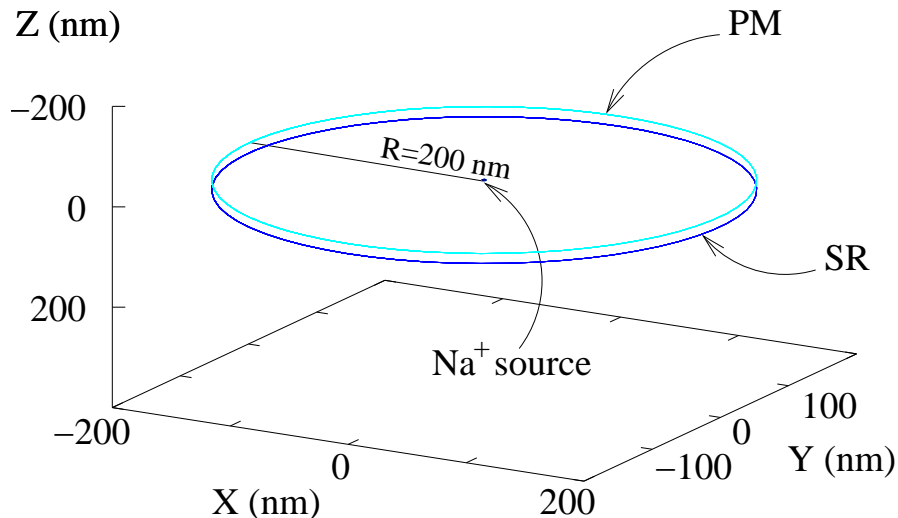


Figure 1: To-scale model nanospace used in the simulations. The separation between the two surfaces (cyan and blue) is 20 nm.

distilled water (30 min). The blocks were then further treated with 1% uranyl acetate for 1 h (*en bloc* staining) followed by three washes with distilled water. Increasing concentrations of ethanol (25, 50, 70, 80, 90 and 95%) were used (10 min each) in the process of gradient dehydration. 100% ethanol and propylene oxide were used (three 10 min washes each) for the final process of dehydration. The blocks were infiltrated in the resin (TAAB 812) and then embedded in molds and polymerized in an oven at 60 °C for 8 h. The embedded blocks were sectioned on a microtome using a diamond knife at the thickness of 80 nm. The sections were then stained with 1% uranyl acetate and Reynolds lead citrate for 4 and 3 min, respectively. Images were obtained with a Phillips 300 electron microscope at 80 kV.

2.2 Simulations

Simulations of Na^+ diffusive motion from a source transporter are based on an implementation of a Monte Carlo random walk (RW), along the lines of methodology previously employed for Ca^{2+} transport simulations[14]. The model nanospace in which the simulations of Na^+ diffusion take place arises from observed physical features and properties of the essential elements for nanodomain signalling. These are either obtained from our laboratory’s studies or from the available literature[16] and they are essentially the TRPC6 cytosolic ‘radius’ and V_{max} [17], the typical dimensions of intracellular nanospace ultrastructure, estimates on the number of pillars, Na^+ diffusivity in cytosol, expected $[\text{Na}^+]$ necessary for NCX reversal (see section 3.1) and during localized Na^+ transients (LNats) observed in [1]. Fig. 1 is a to-scale representation of the geometry of the model nanospace used in the simulations. In the simulations, particles representing Na^+ performs a RW on a cubic lattice with spacing $s = 0.2$ nm; initially picked as an approximation to the expected Na^+ mean free path in water (in turn, as an estimate to the mean free path in cytosol), we also carried out tests for effects of varying this parameter in a previous article and revealed no substantial influence on the results[14]. The RW time step τ was chosen by running several simulations letting

particles cover a predetermined straight line distance d , and recording the number of RW steps N taken to cover d . From diffusion theory, the total time t taken by a random walker in three dimensions to cover the distance d is $t = d^2/(6D_{\text{meas}})$, where D_{meas} is the measured diffusivity of Na^+ in muscle cytosol[18]. The quantity t/N was our choice for τ and its value is 10^{-11} s.

The boundary conditions in our simulations are as follows. At the PM and SR membranes we implemented reflecting conditions: ions arriving at one of those surfaces during their RW are reflected back into the nanospace. At the edges of the model nanospace conditions are perfectly absorbing: ions reaching the lateral boundary of the junction are considered absorbed by the cytosol external to the nanospace, lost from the junctional population and no longer contributing to the PM-SR nanospace concentration, $[\text{Na}^+]_{\text{ns}}$. As explained later, we also positioned a number of obstacles (we refer to them as pillars) to Na^+ motion spanning the distance between the membrane in the nanospace. Pillars behave like elastic scatterers for Na^+ .

Simulation code is written and tested in the C programming language on a computer running a Linux operating system. After testing and troubleshooting, programs are recompiled and run in one of the WestGrid computing nodes[19]. The pseudo-random number generator we used is the algorithm `gsl_rng_m19937` of the GNU Scientific Library[20, 21], since it has sufficient randomness and quality requirements for our purposes. The plots with simulation results were produced using the “freely distributed plotting utility” `gnuplot`[22].

3 Results

3.1 Model foundation

This laboratory has previously experimentally established that a $[\text{Na}^+]$ transient from a NSCC enabled the generation within a PM-SR junctional nanospace of a sufficiently high $[\text{Na}^+]$ gradient to cause NCX reversal[3]. A quantitative estimate of the level of such burst can be obtained by comparing the equilibrium potential of the NCX, E_{NCX} , with the membrane potential, V_{M} , using typical values for vascular smooth muscle cells. These quantities are linked by the equation $E_{\text{NCX}} = V_{\text{M}}$ (where $E_{\text{NCX}} = 3E_{\text{Na}} - 2E_{\text{Ca}}$) between the electrochemical potential of Na^+ (E_{Na}), of Ca^{2+} (E_{Ca}) and the membrane potential (V_{M})[9]. (In general, $E_{\text{C}^{z+}} = RT/(zF) \ln([\text{C}^{z+}]_{\text{out}}/[\text{C}^{z+}]_{\text{in}})$, where R is the universal gas constant, T the absolute temperature, C^{z+} is a z -valent cation, and F is Faraday’s constant.) NCX reversal occurs when $E_{\text{NCX}} < V_{\text{M}}$. We can study this inequality for both resting and activated cell conditions by a plot like the one in Fig. 2. Using for an activated cell $V_{\text{M}} = -20$ mV, $[\text{Na}^+]_{\text{o}} = 140$ mM, $[\text{Ca}^{2+}]_{\text{i}} = 10\mu\text{M}$, $[\text{Ca}^{2+}]_{\text{o}} = 2$ mM, $R = 8.3$ J/(mol K), $T = 310$ K, and $F = 9.65 \times 10^4$ J/(V mol), we observe that, during activation, a $[\text{Na}^+]$ transient of the order of 30 mM or greater is necessary to cause NCX reversal. In this exercise, we have used an estimated value for $[\text{Ca}^{2+}]_{\text{i}} = 10\mu\text{M}$, as that is approximately the lowest value $[\text{Ca}^{2+}]_{\text{i}}$ we expect from observations cited earlier[14].

Now, equipped with **(a)** the fundamental observation of localized $[\text{Na}^+]$ elevation transients in full agreement with the values suggested by the study of Fig. 2[1], **(b)** better knowledge of the identity of NSCC as TRPC6[1, 23], **(c)** the basic idea that the presence of intracellular nanospaces is necessary for this signalplex to be complete, we propose a model

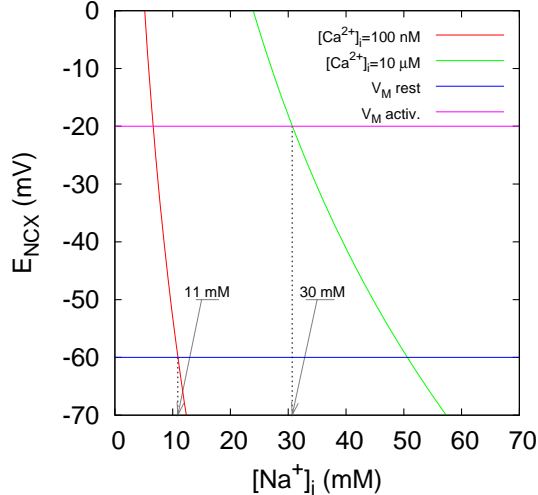


Figure 2: Equilibrium NCX potential in the case of a resting (red curve) or activated (green) smooth muscle cell compared with the corresponding membrane potential, V_M .

to investigate the role of strategic placement of transporters with respect to each other, as well as of a confining membrane and other ionic diffusion limiting structures in the generation within these nanospaces of sufficiently high $[Na^+]_{ns}$ to permit NCX reversal.

The model nanospace used for the study is illustrated in Fig. 1. The dimensions expressed therein are based on high quality EM images showing that the PM-SR separation in these nanospaces is remarkably uniform and about 20 nm. Lateral extension of these closely apposed PM-SR regions is approximately 400 nm (see [14]).

3.2 Random walk simulations: bare PM-SR nanospace

The simplest model nanodomain we studied consists of a shallow cylinder-shaped volume of height $h = 20$ nm and radius $R = 200$ nm, as in Fig. 1. Na^+ entering the nanodomain via an NSCC are represented as particles doing a RW based on a given diffusivity $D = 600 \mu m^2/s$, corresponding to that of Na^+ in muscle cytoplasm as reported in [18]. For simplicity, there is only one Na^+ source positioned at the centre of the PM side of the nanospace (in section 4 we will elaborate further on the issue of the number of Na^+ sources). The simulation programs output the computed $[Na^+]_{ns}$ rise above resting level as a function of time, thereby giving an average $[Na^+]_{ns}$ increase in the nanospace. (From now on $[Na^+]_{ns}$ denotes the increase in cytoplasmic Na^+ concentration in the nanodomain between PM and SR.) Results from this set of simulations are shown in Fig. 3, left panel. This plot helps establish the time scale after which we can consider that the $[Na^+]_{ns}$ has reached a steady-state level. We can observe from the graph that after approximately $100 \mu s$ the concentration has reached a plateau after having increased from zero during an initial transient, as we have explained in the previous section. Having established a time scale for the formation of the approximately maximum level of $[Na^+]_{ns}$, we compute and study the concentration profile inside the junction, by plotting $[Na^+]_{ns}$ as a function of the distance from the Na^+ source. The graph in the right panel of Fig. 3 illustrates a representative result.

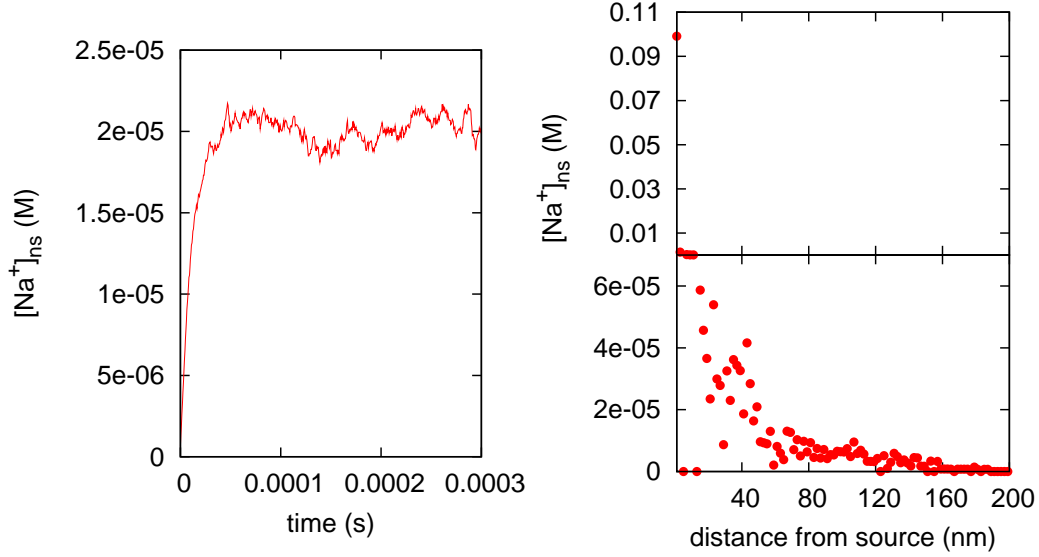


Figure 3: Left panel: $[\text{Na}^+]_{\text{ns}}$ vs t for simplest form of nanospace as in Fig. 1; right panel: $[\text{Na}^+]_{\text{ns}}$ vs distance from Na^+ source placed at the centre of the PM side of the nanospace.

3.3 Random walk simulations: randomly distributed obstacles in the nanospace

Evidently, this simplest incarnation of the model is inadequate to describe the generation of Na^+ transients of the observed size[1], since at steady state elevation of $[\text{Na}^+]_{\text{ns}}$ hovers around 2×10^{-5} M or about three orders of magnitude less than the observed values of 15–20 mM. We need to consider other nanospace features emerging from our ultrastructural images that may be responsible for a larger increase in the $[\text{Na}^+]_{\text{ns}}$. Barring artificially changing the value of Na^+ diffusivity, $[\text{Na}^+]_{\text{ns}}$ can be “forced” to increase if the ions were able to dwell longer in the nanospace than they are in the simple version of the system analyzed so far.

There is convincing evidence suggesting the existence of structures spanning the width of the nanospace and which could constitute an impediment to the free diffusion of Na^+ [2, 24]. Our own observations confirm the existence of electron opaque “pillars” in transmission electron microscopy images like the one in Fig. 4. The size and abundance of these electron opaque structures compares well with the electron dense “bridges” observed by Devine and collaborators in the early ‘70s[24].

Keeping the overall geometry of the model nanospace the same (Fig. 1), we have therefore implemented a number of junction spanning structures in the form of cylindrical pillars, having estimated their size from several images like the one in Fig. 4. From those same images it is possible to approximate the percentage junctional volume occupied by those structures and, in turn, an approximate number of them expected per nanospace. In a series of simulations, we have represented up to 200 pillars randomly distributed within the nanospace (Fig. 5), and then simulated the Na^+ diffusion by a random walk within the pillar-populated nanospace. In this case too, we let the simulations run for a time sufficiently long to ensure that a steady-state level for the $[\text{Na}^+]_{\text{ns}}$ was established. Results are reported in Fig. 6. In all simulations involving random positioning of pillars, to minimize bias from the particular random pillar distribution, we have take average values of the computed $[\text{Na}^+]$

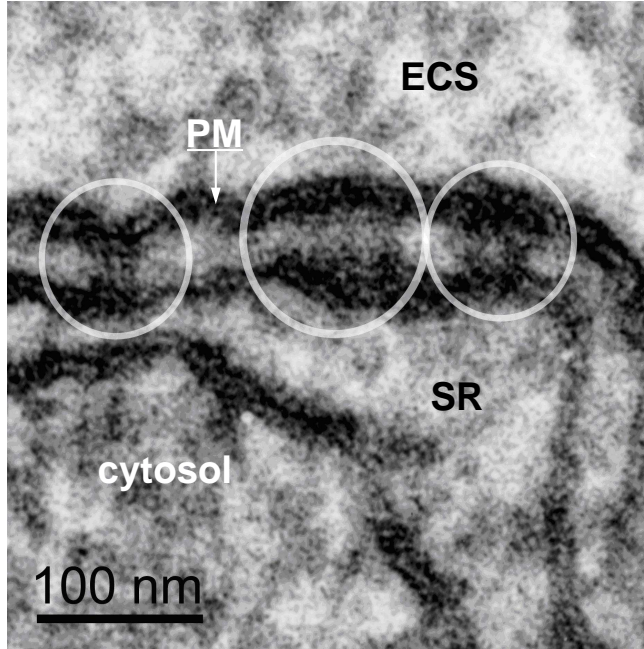


Figure 4: Transmission electron microscopy image showing nanospace bridging electron opaque structures (white circles). Tissue: rabbit inferior vena cava. SR=sarcoplasmic reticulum; PM=plasma membrane; ECS=extracellular space.

over 10 different random pillar distributions. These are the values plotted in the graphs we present in this article.

The results of this series of simulations indicate that having some form of impediment to ionic motion in the junction does produce the effect of increasing the $[\text{Na}^+]_{\text{ns}}$ and of changing its profile to one that decays more slowly with distance from the Na^+ source. We ensured that this effect was not simply a consequence of the decreased nanospace volume due to the presence of the pillars by plotting the steady-state $[\text{Na}^+]$ computed with different numbers of pillars in the junction (blue dots in Fig. 7) and comparing it with an increase in $[\text{Na}^+]$ merely due to reducing the nanospace volume by the volume of the pillars (red line in Fig. 7). The plot in Fig. 7 demonstrates that ion collisions with pillars do indeed have a role in forcing Na^+ to dwell longer in the nanospace.

3.4 Random walk simulations: non-randomly distributed obstacles

Clearly, the presence of obstacles to diffusion has an effect of increasing $[\text{Na}^+]_{\text{ns}}$, however the values we obtain this way are not yet comparable with those measured during the local $[\text{Na}^+]$ elevation transients. Other junctional features need to be accounted for in order to understand the mechanism giving rise to such high Na^+ transients necessary to reverse the NCX and observed by Poburko and coworkers[1]. We considered the hypothesis that nature might place these obstacles “strategically” rather than randomly, in a neighbourhood of a Na^+ source, so as to favour the generation of the gradients needed to drive the signalling chain. The rationale is that while a random set of pillars does show an ability to retain ions

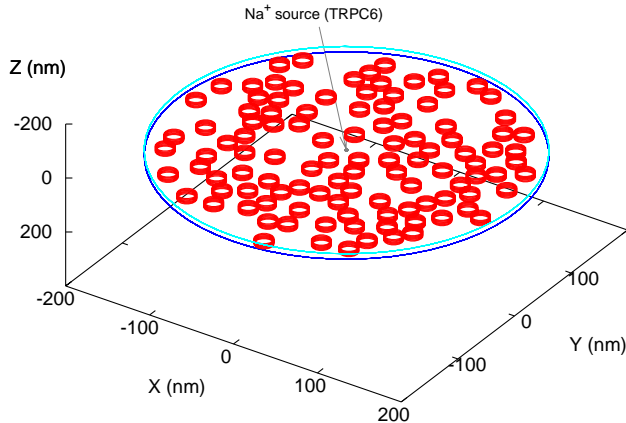


Figure 5: To-scale model nanospace including about 200 10-nm radius randomly placed cylindrical pillars spanning the distance between the two surfaces.

in the nanospace longer and therefore allow higher concentration build up, it does not do it efficiently enough to quantitatively account for the observed $[\text{Na}^+]_{\text{ns}}$ transients. We then ran some simulations in which pillars are placed in a circle around a Na^+ source in such a way that we can control the porosity of this pillar fence to the passage of random walking ions. (Imagining to stand where the Na^+ source is, the circle of pillars would appear as a 20-nm-high set of slabs surrounding the source itself, with thin rectangular gaps between the slabs; with this in mind, porosity is defined as the ratio of the entire surface area of the gaps to that of the slabs plus gaps.) The configuration of our model nanospace in this case is shown in Fig. 8, as a two dimensional x,y -projection.

Representative results from these simulations are reported in Fig. 9. The dramatic increase in the $[\text{Na}^+]_{\text{ns}}$ in the vicinity of the source caused by this type of obstacle configuration is immediately evident. $[\text{Na}^+]_{\text{ns}}$ is in this case of the same order of magnitude as the observed localized $[\text{Na}^+]$ transient elevation phenomenon[1]. Note furthermore that in this configuration the model suggests that the time for the $[\text{Na}^+]_{\text{ns}}$ to reach steady-state is much longer than in the case of random distribution of pillars. The more scattered data in the plot of the right panel in Fig. 9 are due to the fact that the system in this case has yet to reach equilibrium.

4 Discussion

The stochastic computational model presented herein attempts to give a quantitative description of the mechanism behind the observed localized $[\text{Na}^+]$ transients observed in VSMC[1]. Based as much as feasible on experimental observations of the physical and physiological features of the intracellular nanospaces in which these transients are hypothesized to occur, the model results lead us to conclude that $[\text{Na}^+]$ can build to sufficiently high values in PM-SR junctions to give rise to the observed transients.

Three main steps lead to the fundamental hypothesis behind this work. The first stems from earlier work by this laboratory elucidating the sequence leading to asynchronous Ca^{2+} oscillations in VSMC[1, 14]. Succinctly, a large external Na^+ influx causes the reversal of the NCX and consequent Ca^{2+} entry to refill the SR after SR-Ca^{2+} release via IP_3R channels

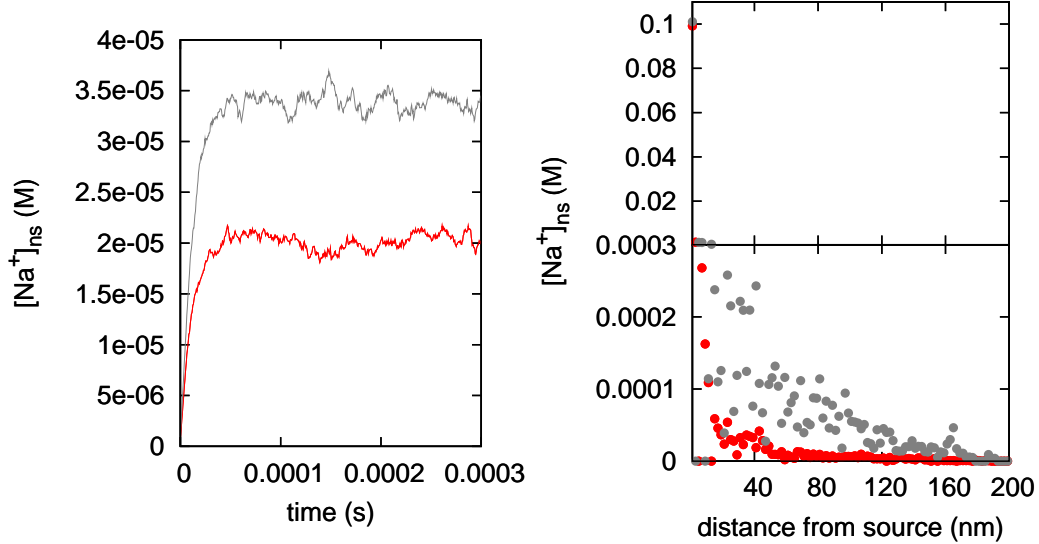


Figure 6: $[\text{Na}^+]_{\text{ns}}$ within a model nanospace containing a number of pillars occupying about 30% of the volume, as in Fig. 5. Left panel: computed $[\text{Na}^+]_{\text{ns}}$ as a function of time; the values of $[\text{Na}^+]_{\text{ns}}$ in this graph are an average across the entire nanospace. Right panel: concentration profile within nanospace. The red curve and dots are the same data displayed in Fig. 3.

upon cell stimulation provokes contraction. The second is the observation of two main features of the localized $[\text{Na}^+]_{\text{ns}}$ elevation transients[1]: they appear as a punctate pattern on the periphery of VSMC (with puncta having a given time course), and their peak $[\text{Na}^+]_{\text{ns}}$ values are comparable to the $[\text{Na}^+]_{\text{i}}$ values necessary to cause NCX reversal (see Fig. 2 and relevant text). Thirdly, our previously published model supports the idea that NCX reversal-mediated Ca^{2+} entry in PM-SR nanospaces introduces sufficient Ca^{2+} to refill the SR during asynchronous Ca^{2+} waves[14]. Based on these three points, the hypothesis we set out to study with our model is that the observed localized $[\text{Na}^+]_{\text{ns}}$ transients occur in PM-SR nanodomains (or nanospaces or junctions), in other words, that in those junctions, due to Na^+ influx via a TRPC6 channel, $[\text{Na}^+]_{\text{ns}}$ can attain levels, that cause Ca^{2+} entry via NCX reversal.

Simulation results from our simplest version of model (Fig. 3), namely, a PM-SR nanospace filled with cytosol (represented in our simulations by the diffusivity of Na^+) with only one TRPC6 channel as Na^+ source suggest that this simple view is not adequate to describe the formation of $[\text{Na}^+]_{\text{ns}}$ transients. This is mainly due to the large value of the diffusion coefficient of Na^+ , which is about three times that of free Ca^{2+} in cytosol, and the fact that there is no observed buffering effect of Na^+ in cytosol[18]. Recent $[\text{Na}^+]_{\text{ns}}$ measurements in isolated rabbit ventricular myocytes by Despa and Bers ([25, 26]) also suggest that the effective diffusivity of Na^+ may be much slower than the one found by Kushmerick and Podolsky[18], although no explanation as to the mechanism behind it was suggested. In [25], among other things, Despa and Bers measured endogenous Na^+ buffering in cytosol and found it negligible when compared to that of other important species like Ca^{2+} , for example. It is well known that Ca^{2+} buffering lowers its diffusivity dramatically[27, 28], thus possibly contributing to easier generation of Ca^{2+} gradients in confined spaces like the PM-SR nanospaces. Presum-

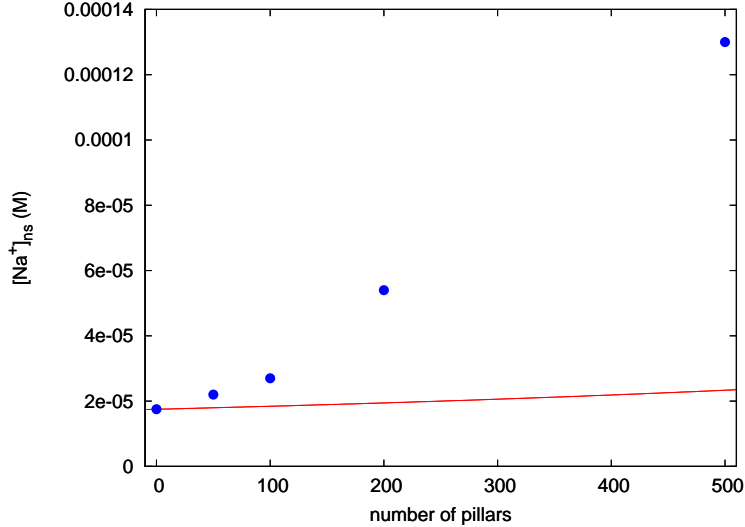


Figure 7: Comparison of steady-state Na^+ calculated only accounting for the volume effect of pillars in the nanospace (red line) and computed from the simulations (blue dots).

ing the slight Na^+ buffering effect observed in cardiac cell cytosol is mirrored in smooth muscle cells, it clearly could not provide sufficient slowing down of Na^+ diffusivity to aid local transient creation. It seems instead ever more plausible that it must be some sort of physical obstruction to ionic motion that gives rise to a slower effective diffusivity for Na^+ . We then considered that physical obstructions to ionic motion can have the overall effect of increasing the time spent by each Na^+ in the nanospace thereby increasing the value of $[\text{Na}^+]_{\text{ns}}$. Ever since first reported measurement of Na^+ diffusivity in muscle cells[18], it was hinted that it is physical rather than chemical interactions that cause a retardation of the ionic (and non-ionic for that matter—sorbitol and sucrose specifically) intracellular diffusion. Our ultrastructural observations of nanospace spanning electron opaque structures support this idea (Fig. 4) and agree fully with earlier reports of similar structures in SMC[24]. The introduction of such physical obstruction in the simulations seems then more than warranted and very plausible. Moreover, if the “tortuosity factor”, introduced by Kushmerick, arising from physical interaction is indeed important in the bulk cytosol, then it would be even more so in the restricted PM-SR nanospaces. While the introduction of physical obstacles to ionic motion in our simulations does produce higher $[\text{Na}^+]_{\text{ns}}$ gains (Fig. 6 and 7), to obtain a quantitative agreement with the observed level of $[\text{Na}^+]$ during the transients we need to hypothesize further that these junction spanning structures are not distributed at random, but rather form an organized barrier around a given Na^+ source within the nanospace. Our simulation results in this case (Fig. 9) agree quantitatively with the observed $[\text{Na}^+]$ transients, giving a Na^+ of the same order of magnitude as the experimental measurements. The left panel plot in Fig. 9 also shows that the $[\text{Na}^+]$ with this configuration of pillars will reach steady state with a time constant that is at least ten times longer than in the case of randomly distributed pillars. This is another feature supporting our hypothesis that these transients are formed in the PM-SR nanospaces with the aid of a relatively tight fence of pillars around the Na^+ source. In fact, the measured transients are reported to be very long lived with a ramp up time to steady state of about 30 s, a time scale that the simpler versions

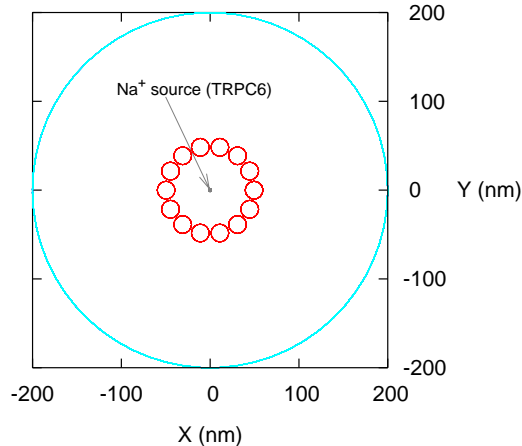


Figure 8: To-scale x,y -projection of model nanospace including 14 10-nm-radius cylindrical pillars positioned in a 5-nm-radius ring around a Na^+ source in the centre, thereby giving a 1% porosity for ion passage.

of the model could not reproduce at all.

It therefore appears that two features are essential if these transients must occur within PM-SR nanospaces: there must be physical obstructions to Na^+ motion, forming an organized barrier around each Na^+ source (TRPC6 channels) *and* NCX must be localized near a TRPC6 within such barrier to be able to sense the high $[\text{Na}^+]$, reverse and allow Ca^{2+} entry. The second of these two features is suggested by a number of observations. There are studies supporting the idea that TRPC channels and $\text{Na}^+/\text{Ca}^{2+}$ exchangers are functionally and physically linked and form an important signalplex in several different systems[29]. Still other studies indicate that at least certain kinds of TRP channels are found in close proximity of caveolin[30, 31]. Combined with our earlier observations that NCX tend to crowd near the necks of caveolae[14], this makes a strong case for a physical association between TRP channels and NCX. The first of the above mentioned desirable features—patterns of physical obstructions within the nanodomains—is a harder matter to study experimentally and one of the current/future directions our laboratory is following.

To further study the issue of the localized $[\text{Na}^+]$ transient duration requires more computationally demanding simulations, which we are currently tackling. We can however make a qualitative argument to suggest how the time scale of the observed transients can also be supported by our model. We have so far only implemented one Na^+ source, or one TRPC6 channel. However, we have observed earlier that during activation of rabbit inferior vena cava SMC there could be about 16 NCX in the junctions[14]. If we conjecture that TRPC6 and NCX must be in physical proximity, as we speculated above, it is consistent to assume that there may be more than one TRPC6 in each junction functioning as a Na^+ entry gate, and perhaps even as many as there are NCX.

Other transporters such as NCX and Na^+/K^+ ATPases (NKA) certainly also play a role in shaping the PM-SR nanodomain $[\text{Na}^+]$ profiles that drive NCX-mediated Ca^{2+} entry during VSMC activation. In the simple model we presented in this article, we focussed on the role of TRPC6 since it is by far the larger capacity transporter of the TRPC6, NCX, NKA trio (millions of ions per second, hundreds per second and tens per second, respectively). This first approximations quantitative model supports the idea that localized

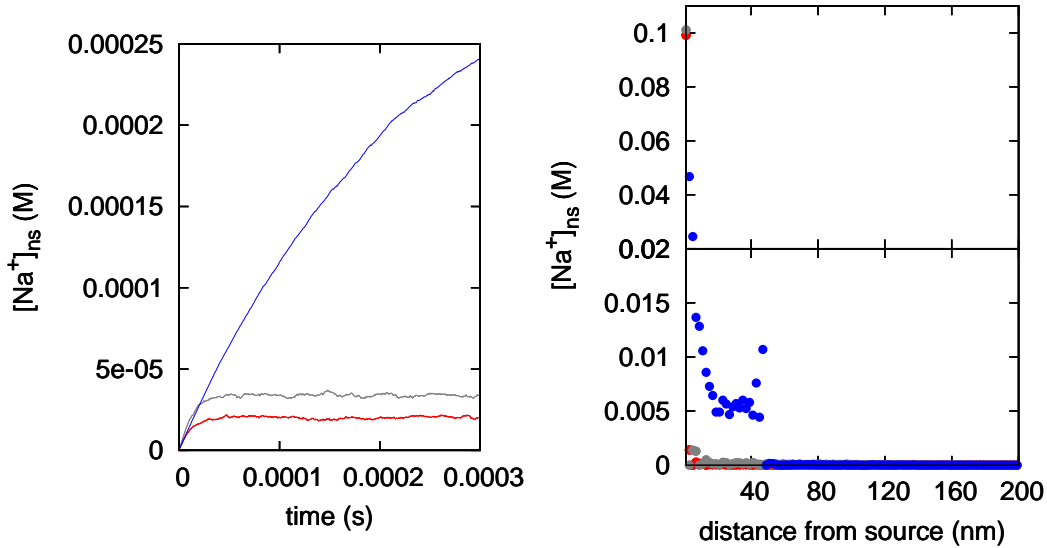


Figure 9: $[\text{Na}^+]_{\text{ns}}$ within a model nanospace containing 14 pillars “strategically” positioned around a Na^+ source at the centre and making a 1% porous fence, as in Fig 8. Left panel: computed $[\text{Na}^+]_{\text{ns}}$ as a function of time. Right panel: concentration profile within nanospace at $t = 0.0003$ s. The red and the grey curves and dots refer to data displayed in Fig. 3 and 6.

$[\text{Na}^+]$ elevation transients take place at PM-SR nanodomains and strongly suggests that physical impediment to ionic mobility of Na^+ is also a necessary factor for their generation.

Acknowledgments

The research was supported by grants from the Canadian Institute of Health Research and the Heart and Stroke Foundation of British Columbia and Yukon. This project has been enabled by the use of WestGrid computing resources, which are funded in part by the Canada Foundation for Innovation, Alberta Innovation and Science, BC Advanced Education, and the participating research institutions. WestGrid equipment is provided by IBM, Hewlett Packard and SGI.

References

- [1] Damon Poburko, Chiu-Hsiang Liao, Virginia S Lemos, Eric Lin, Yoshiaki Maruyama, William C Cole, and Cornelis van Breemen. Transient receptor potential channel 6-mediated, localized cytosolic $[\text{na}^+]$ transients drive $\text{na}^+/\text{ca}^{2+}$ exchanger-mediated ca^{2+} entry in purinergically stimulated aorta smooth muscle cells. *Circ Res*, 101(10):1030–1038, Nov 2007.
- [2] Damon Poburko, Nicola Fameli, Kuo-Hsing Kuo, and Cornelis van Breemen. Ca^{2+} signaling in smooth muscle: *Trpc6*, *ncx* and *lnats* in nanodomains. *Channels (Austin)*, 2(1):10–12, 2008.

- [3] C. H. Lee, D. Poburko, P. Sahota, J. Sandhu, D. O. Ruehlmann, and C. van Breemen. The mechanism of phenylephrine-mediated $[Ca^{2+}]_i$ oscillations underlying tonic contraction in the rabbit inferior vena cava. *J Physiol*, 534(Pt 3):641–650, Aug 2001.
- [4] H. T. Syyong, H. H C Yang, G. Trinh, C. Cheung, K. H. Kuo, and C. van Breemen. Mechanism of asynchronous Ca^{2+} waves underlying agonist-induced contraction in the rat basilar artery. *Br J Pharmacol*, 156(4):587–600, Feb 2009.
- [5] Shen Zhang, Hui Dong, Lewis J Rubin, and Jason X-J Yuan. Upregulation of Na^+/Ca^{2+} exchanger contributes to the enhanced Ca^{2+} entry in pulmonary artery smooth muscle cells from patients with idiopathic pulmonary arterial hypertension. *Am J Physiol Cell Physiol*, 292(6):C2297–C2305, Jun 2007.
- [6] M. Teubl, K. Groschner, S. D. Kohlwein, B. Mayer, and K. Schmidt. Na^+/Ca^{2+} exchange facilitates Ca^{2+} -dependent activation of endothelial nitric-oxide synthase. *J Biol Chem*, 274(41):29529–29535, Oct 1999.
- [7] Magdalena M Szewczyk, Kim A Davis, Sue E Samson, Fiona Simpson, Patangi K Rangachari, and Ashok K Grover. Ca^{2+} -pumps and Na^+-Ca^{2+} -exchangers in coronary artery endothelium versus smooth muscle. *J Cell Mol Med*, 11(1):129–138, 2007.
- [8] M. A. Nazer and C. Van Breemen. A role for the sarcoplasmic reticulum in Ca^{2+} extrusion from rabbit inferior vena cava smooth muscle. *Am J Physiol*, 274(1 Pt 2):H123–H131, Jan 1998.
- [9] M. P. Blaustein and W. J. Lederer. Sodium/calcium exchange: its physiological implications. *Physiol Rev*, 79(3):763–854, Jul 1999.
- [10] N. Zhong, V. Beaumont, and R. S. Zucker. Roles for mitochondrial and reverse mode Na^+/Ca^{2+} exchange and the plasmalemma Ca^{2+} atpase in post-tetanic potentiation at crayfish neuromuscular junctions. *J Neurosci*, 21(24):9598–9607, Dec 2001.
- [11] Elena Germinario, Alessandra Esposito, Menotti Midrio, Samantha Peron, Philip T Palade, Romeo Betto, and Daniela Danieli-Betto. High-frequency fatigue of skeletal muscle: role of extracellular Ca^{2+} . *Eur J Appl Physiol*, 104(3):445–453, Oct 2008.
- [12] P. C. Levesque, N. Leblanc, and J. R. Hume. Role of reverse-mode Na^+-Ca^{2+} exchange in excitation-contraction coupling in the heart. *Ann N Y Acad Sci*, 639:386–397, 1991.
- [13] Cheng-Han Lee, Kuo-Hsing Kuo, Jiazhen Dai, Joyce M Leo, Chun Yong Seow, and Cornelis van Breemen. Calyculin-a disrupts subplasmalemmal junction and recurring Ca^{2+} waves in vascular smooth muscle. *Cell Calcium*, 37(1):9–16, Jan 2005.
- [14] Nicola Fameli, Cornelis van Breemen, and Kuo-Hsing Kuo. A quantitative model for linking Na^+/Ca^{2+} exchanger to serca during refilling of the sarcoplasmic reticulum to sustain $[Ca^{2+}]_i$ oscillations in vascular smooth muscle. *Cell Calcium*, 42(6):565–575, Dec 2007.

- [15] K. H. Kuo, L. Wang, P. D. Par, L. E. Ford, and C. Y. Seow. Myosin thick filament lability induced by mechanical strain in airway smooth muscle. *J Appl Physiol*, 90(5):1811–1816, May 2001.
- [16] Cheng-Han Lee, Damon Poburko, Kuo-Hsing Kuo, Chun Yong Seow, and Cornelis van Breemen. Ca(2+) oscillations, gradients, and homeostasis in vascular smooth muscle. *Am J Physiol Heart Circ Physiol*, 282(5):H1571–H1583, May 2002.
- [17] A. Dietrich and T. Gudermann. Trpc6. *Handb Exp Pharmacol*, (179):125–141, 2007.
- [18] M. J. Kushmerick and R. J. Podolsky. Ionic mobility in muscle cells. *Science*, 166(910):1297–1298, Dec 1969.
- [19] <http://westgrid.ca>.
- [20] M. Galassi J. Davies J. Theiler B. Gough G. Jungman P. Alken M. Booth F. Rossi. *GNU Scientific Libraries Reference Manual (2nd Ed.)*. 2006.
- [21] <http://www.gnu.org/software/gsl/>.
- [22] <http://www.gnuplot.info>.
- [23] Virginia S Lemos, Damon Poburko, Chiu-Hsiang Liao, William C Cole, and Cornelis van Breemen. Na+ entry via trpc6 causes ca2+ entry via ncx reversal in atp stimulated smooth muscle cells. *Biochem Biophys Res Commun*, 352(1):130–134, Jan 2007.
- [24] C. E. Devine, A. V. Somlyo, and A. P. Somlyo. Sarcoplasmic reticulum and excitation-contraction coupling in mammalian smooth muscles. *J Cell Biol*, 52(3):690–718, Mar 1972.
- [25] Sanda Despa and Donald M Bers. Na/k pump current and [na](i) in rabbit ventricular myocytes: local [na](i) depletion and na buffering. *Biophys J*, 84(6):4157–4166, Jun 2003.
- [26] Sanda Despa, Jens Kockskemper, Lothar A Blatter, and Donald M Bers. Na/k pump-induced [na](i) gradients in rat ventricular myocytes measured with two-photon microscopy. *Biophys J*, 87(2):1360–1368, Aug 2004.
- [27] N. L. Allbritton, T. Meyer, and L. Stryer. Range of messenger action of calcium ion and inositol 1,4,5-trisphosphate. *Science*, 258(5089):1812–1815, Dec 1992.
- [28] J. Wagner and J. Keizer. Effects of rapid buffers on ca2+ diffusion and ca2+ oscillations. *Biophys J*, 67(1):447–456, Jul 1994.
- [29] Petra Eder, Michael Poteser, Christoph Romanin, and Klaus Groschner. Na(+) entry and modulation of na(+)/ca(2+) exchange as a key mechanism of trpc signaling. *Pflugers Arch*, 451(1):99–104, Oct 2005.

- [30] T. Lockwich, B. B. Singh, X. Liu, and I. S. Ambudkar. Stabilization of cortical actin induces internalization of transient receptor potential 3 (trp3)-associated caveolar ca^{2+} signaling complex and loss of ca^{2+} influx without disruption of trp3-inositol trisphosphate receptor association. *J Biol Chem*, 276(45):42401–42408, Nov 2001.
- [31] So-Ching W Brazer, Brij B Singh, Xibao Liu, William Swaim, and Indu S Ambudkar. Caveolin-1 contributes to assembly of store-operated ca^{2+} influx channels by regulating plasma membrane localization of trpc1. *J Biol Chem*, 278(29):27208–27215, Jul 2003.